Science of the Total Environment 729 (2020) 138803

Contents lists available at ScienceDirect

Science of the Total Environment

journal homepage: www.elsevier.com/locate/scitotenv

Salt intrusion alters nitrogen cycling in tidal reaches as determined in field and laboratory investigations

Rongrong Xie [a,b,c], Peiyuan Rao [a], Yong Pang [d], Chengchun Shi [e], Jiabing Li [a,b,*], Dandan Shen [f,g,**]

[a] College of Environmental Science and Engineering, Fujian Normal University, Fuzhou 350007, China
[b] Key Laboratory of Pollution Control and Resource Recycling of Fujian Province, Fujian Normal University, Fuzhou 350007, China
[c] Section of Physical Oceanography and Instrumentation, Leibniz Institute for Baltic Sea Research, Warnemuende, D-18119 Rostock, Germany
[d] College of Environment, Hohai University, Nanjing 210098, China
[e] Fuzhou Research Academy of Environmental Sciences, Fuzhou 350013, China
[f] Section of Biological Oceanography, Leibniz Institute for Baltic Sea Research, Warnemuende, D-18119 Rostock, Germany
[g] Department of Ecology, Environment and Plant Sciences, Stockholm University, 106 91 Stockholm, Sweden

HIGHLIGHTS

- Elevated salinity led to increases in NH_4^+ mainly via stimulated dissimilatory nitrate reduction to ammonium (DNRA).
- Decreased nitrification and increased DNRA decreased NO_3^- at high salinity.
- An increase in salinity promoted dissolved N_2O accumulation during denitrification.
- Salinity changes accompanied with redox oscillations reduce nitrification but enhance denitrification and DNRA.

GRAPHICAL ABSTRACT

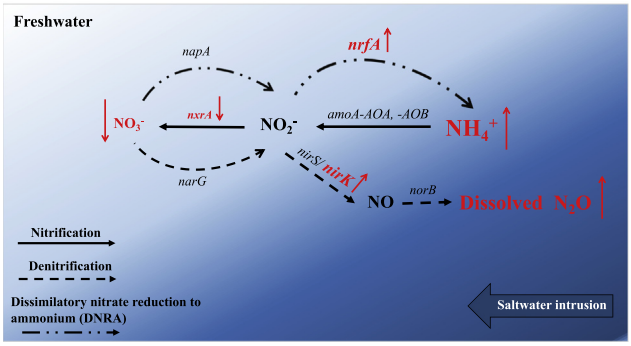

ARTICLE INFO

Article history:
Received 20 February 2020
Received in revised form 6 April 2020
Accepted 17 April 2020
Available online 25 April 2020

Editor: Frederic Coulon

Keywords:
Nitrogen cycle
Salt intrusion
Functional genes
Field monitoring
Microcosms

ABSTRACT

Salinization is a growing problem throughout the world and poses a threat especially to freshwater ecosystems. However, much remains to be learned about the mechanisms by which salinity impacts microbially mediated biogeochemical processes. Elevated nitrogen (N) concentrations in estuarine ecosystems have led to their eutrophication, but the relationship between N transformation and the functional genes involved in the response to saltwater intrusion is poorly understood. Here, using the Minjiang River, a tidal river in southeastern China as an easily accessible natural laboratory, we conducted a 2-year field survey to investigate N speciation during ebb and flood tides. Then, in a laboratory experiment we simulated the varying degrees of salt intrusion that occur in natural tidal reaches. The microcosm study allowed quantitative assessments of N transformation and functional gene responses. The field surveys showed that concentrations of NH_4^+ rose during flood tides, while the concentrations of NO_3^- and total N fluctuated. In the microcosms, NO_3^- concentrations decreased in response to salt pulses, due to simultaneous declines in the abundance of genes responsible for nitrification and increases in the abundance of those involved in dissimilatory nitrate reduction to ammonium (DNRA). The elevated salinity led to increased yields of NH_4^+, a response that correlated positively with the abundance of *nrfA* genes, involved in DNRA. Furthermore, an increase in salinity promoted N_2O accumulation during the denitrification

* Correspondence to: J. Li, 8 Shangsan Rd, Fuzhou 350007, China.
** Correspondence to: D. Shen, Department of Ecology, Environment and Plant Sciences, Stockholm University, 106 91 Stockholm, Sweden.
E-mail addresses: lijiabing@fjnu.edu.cn (J. Li), dand.shen@gmail.com (D. Shen).

https://doi.org/10.1016/j.scitotenv.2020.138803

process. Altogether, our study suggests that saltwater intrusion leads to a decrease in nitrification while favoring N transformation via denitrification and DNRA and that N_2O accumulation in the water is dependent on the strength of the salt pulse.

1. Introduction

Saltwater intrusion, i.e., the movement of saline water into freshwater aquifers, is among the consequences of rising global sea levels and the damming of many waterways (Barlow and Reichard, 2010; Church et al., 2013; Alcérreca-Huerta et al., 2019). It is a growing problem in many countries, including the USA, Mexico, Canada and China. Moreover, salinity is a key driver of nitrogen (N) cycling, and elevated N concentrations in aquatic systems can lead to undesirable shifts in microbial community structure, the development of harmful algal blooms, a decrease in the oxygen content, and the contamination of drinking water (Camargo and Alonso, 2006). Nitrate (NO_3^-) and ammonium (NH_4^+) are among the most widely measured analytes and they account for 85% of total N (TN) in coastal waters, including estuarine waters and coastal rain, based on volume-weighted averages (Kieber et al., 2005).

Investigations into the impact of salinity on N processes in aquatic systems have largely focused on their sediments, rather than their water (Mcclung and Frankenberger, 1985; Osborne et al., 2015; Hu et al., 2016; Xie et al., 2017a). Studies of N cycling in natural waters are complicated by the varying hydrological dynamics of natural waters. In estuaries change in the speciation of the main N species in response to changes in salinity have been reported by some authors (Jia, 2011; Helali et al., 2016) while others found no evidence of distinct patterns in the concentrations of NH_4^+ and NO_3^- during a tidal event accompanied by a drastic change in salinity (Rahaman et al., 2013). In other cases, real-time monitoring demonstrated a strong inverse correlation between salinity and NO_X, total inorganic N (TIN) and total dissolved N (Ribas-Ribas et al., 2011; Das et al., 2017; Wang et al., 2017). These studies do not reveal a consistent response of N speciation to changes in salinity, which could have been attributed to temporal and spatial variations of N speciation. Thus, when possible, studies should measure and report temporal and spatial patterns of N speciation in the same environmental context, allowing the results to be comparable. Yet, how the pattern of N speciation following salinity change varies depending on the character and the strength of salinity fluctuation remains unclear.

Nitrification, denitrification and dissimilatory nitrate reduction to ammonium (DNRA) are main N transforming processes during the N-cycle and are functionally connected (Santoro et al., 2008; Santoro, 2010; Kim et al., 2017; Pang et al., 2019). Nitrification is a two-step microbial process usually performed by two distinct functional groups of aerobic chemoautotrophic microorganisms (Santoro, 2010). Aerobic ammonia oxidation is the first step of nitrification where NH_4^+ is oxidized into NO_2^- by ammonia-oxidizing bacteria and archaea (AOB and AOA, correspondingly) that carry ammonia monoxygenase (*amoA*) gene (Shen et al., 2012). Then, oxidization of nitrite into nitrate is the second step of nitrification and is performed mainly by nitrite-oxidizing bacteria (NOB) that carry *nxrA* gene. Unlike nitrification, denitrification typically occurs under anoxic conditions (Giblin et al., 2010; Giblin et al., 2013; Zhou et al., 2017). However, few studies have reported the occurrence of aerobic denitrification in freshwater ecosystems (Coban et al., 2015) and in marine sediments (Gao et al., 2010). Denitrification process encompasses the reduction of NO_3^- through NO_2^- to nitric oxide (NO), which then produces nitrous oxide (N_2O) and finally N_2, in which nitrite reductase genes *nirK* and *nirS*, nitric oxide reductase gene *norB* and nitrous oxide reductase gene *nosZ* are involved.

Numerous studies have shown that NO_3^- plays a crucial role in nitrification-denitrification coupling (Giblin et al., 2010; Xia et al., 2017). In addition, aerobic nitrification provides NO_2- and NO_3^- for the denitrification and DNRA, but it also competes with the anaerobic ammonia oxidation for to NH_4^+ (Kim et al., 2017). DNRA represents an alternative pathway to the reduction of NO_3^- and/or NO_2^- to NH_4^+, which requires *napA* and *nrfA* genes for nitrate/nitrite ammonification. Accordingly, both the denitrification and DNRA require NO_3^- reduction and compete for NO_3^- as an electron acceptor in low-oxygen environments. The importance of environmental conditions that govern this competition and the end product of bacterial nitrate respiration is discussed, including supply of nitrite relative to nitrate (Kraft et al., 2014), temperature (Dong et al., 2011) and pH (Schmidt et al., 2011). Few existing studies have implied that the higher rates of DNRA are associated with higher salinity, while lower salinity favors high rates of denitrification (Giblin et al., 2010). DNRA-performing bacteria have competitive advantages over denitrifiers in estuaries that are likely to experience salinity and nitrate fluctuations (Smith et al., 2015). Both field (Giblin et al., 2010; Osborne et al., 2015) and laboratory (Laverman et al., 2007; Li et al., 2014) studies have consistently shown that nitrification and denitrification in sediments are depressed at higher salinities whereas the rate of DNRA increases. Moreover, saltwater intrusion may support DNRA (Laverman et al., 2007). Nevertheless, the interrelationships among the N reactions are extremely complex and the potential entanglement complicates the identification of causal relationships. Therefore, it is important to explicitly elucidate the relationships of these N transformation processes in aquatic environments that experience salinity fluctuation, especially from a microbial perspective, to understand the mechanisms by which saltwater intrusion affects N cycle.

The community composition of organisms responsible for N cycling is also sensitive to salinization (Santoro, 2010). Increases in salinity inhibit the activity of nitrifying bacteria (Rysgaard et al., 1999), alter the seasonal pattern of DNRA communities and lead to lower denitrification rates (Giblin et al., 2010). The community structure of ammonia-oxidizing archaea and/or bacteria positively correlated with salinity (Wang et al., 2018), while in other studies an inverse correlation was found (Sanders and Laanbroek, 2018). For denitrifying communities, the abundance of *nirK* negatively correlated with salinity (Wang et al., 2018), whereas that of *nirS* positively correlated with salinity (Franklin et al., 2017). Similarly, the higher abundance of *nrfA* gene required for DNRA tended to correlate with increasing salinity (Franklin et al., 2017). These observations underscore the need to clarify the correlation of N-related functional genes and changing salinity (Stoliker et al., 2016; Damashek and Francis, 2018; Pang et al., 2019), and thus to pinpoint the dominant genes of nitrification, denitrification and DNRA that govern the end product during N cycling.

Tidal reaches have the features of both an estuary and a river, which account for their changeable freshwater-brackish environments. Due to their dual directional flow and downward bottom slope, tidal reaches harbor diverse microbial populations. The drastic salinity changes that occur in tidal reaches between the flood tide and the ebb tide make these systems ideal natural laboratories to study the effects of salinity on microbially mediated N speciation (Xie et al., 2017b). Therefore, we conducted a number of field investigations aimed at answering the question whether salinity intrusions between flood tides and ebb tides in a tidal reach alter the concentrations of the different N forms, including NH_4^+, NO_3^-, and TN. In the fields, saltwater intrusion usually occurs in the setting of a change in environmental conditions. Thus, to explicitly examine the impact of changing salinity on variability of N speciation and N-related functional genes, we set up a controlled microcosm study in the lab in which periodic saltwater intrusions of the natural

river water were mimicked by salt pulses. The microbial community size that developed in response to the experimental manipulation was assessed in a 16S rRNA survey. In addition, the abundances of a select set of functional genes (nitrification: *amoA-AOA, -AOB and nxrA*, denitrification: *narG*, *nirK*, *nirS* and *norB*, and DNRA: *napA* and *nrfA*) and their correlation with N transformation (NH_4^+, NO_3^-, and dissolved N_2O) following salinity pulse were determined.

2. Materials and methods

2.1. Research area

The study area was the Minjiang River of southeastern China and specifically its tidal reach (Fig. 1). The Minjiang River is a largely regulated river, with controlled flow conditions that lead to recurrent salinity intrusion events. The upstream discharge is dominated by the Shuikou Dam and the minimum ecological discharge is 308 m^3/s (Xie et al., 2017b). In recent years, severe saltwater intrusions have led to a degradation of the drinking water quality such that the water plant has had to abruptly cut off the water supply on several occasions.

2.2. Field surveys

Five field surveys on nitrogen speciation were conducted in December 2013, April, May, and August 2016 and January 2017 to investigate the effect of saltwater intrusion on nitrogen speciation, because the occurrence of frequent salinity intrusion in the Minjing River during those years has been reported (Xie et al., 2017b). In 2013, NH_4^+, NO_3^- and TN were measured every 2-h but in 2016–2017, water samples were collected during ebb tide and flood tide. According to the Chinese standard (GB3838-, 2002), the maximum allowable concentration of NH_4^+ and TN in water is 1.0 mg/L, but there is no standard for the maximum concentration of NO_3^- (GB3838-, 2002). Our survey results showed that NH_4^+ increased and NO_3^- decreased during saltwater intrusions (Supplementary Fig. S1). According to the outcome of salinity changes observed from those field surveys (Supplementary Table S1), we found that salinity changes appeared to be stronger for summer's investigations, i.e., August, indicating potential evaporation due to warm temperature might have caused a drastic fluctuation in salinity. Therefore, two consecutive surveys were conducted, on 30 August 2017 and 22 August 2018, in order to extend previous field investigations and most importantly to explicitly investigate the impact of salt intrusion on N speciation in the tidal reach. Langqi Bridge (station S1), Jingangtui (station S2) and Wulongjiang (station S3) were chosen as the study sites because while they are highly salt-impacted they also differ in their magnitude of salt intrusion (decreasing from downstream to upstream) (Fig. 1). Thus, S1 and S2 are regularly subjected to salt intrusion, while S3 is replenished with freshwater but is otherwise saltier following extreme tidal events (Pan et al., 2015). Together, the three sites provided an ideal ecosystem to study the effect of salinity changes on water chemistry and microbially mediated N-related processes.

Salinity was monitored using a salinometer (CT-3081, Kedida, China). The accuracy of the salinity measurements was within 0.02. In the UNESCO (1985) definition, the practical salinity scale is a conductivity ratio and thus has no units. In our study, all salinities are reported according to this scale and therefore without units. The average tidal range in the area of Minjiang Estuary is 4.5 m, but the maximum range can exceed 6 m (Xie et al., 2017b). Previous saltwater intrusions into Minjiang Estuary resulted in salinity stratification in the study area. Hence, we employed a strategy of sampling different depths in order to more accurately determine N concentrations over the whole cross-section of each station compared to measurements at single depths. To account for fluctuations in the water level in the tidal reach areas and to obtain a thorough determination of N speciation, three (S2 in 2017) or four (S2 in 2018) or two (S1 in 2018) samples were collected from each station at 2-h intervals depending on the depth of the station sampled. Sample handling for the N speciation analyses was conducted according to the instructions in 'Water quality—Technical regulation of the preservation and handling of samples' (HJ493-, 2009). Briefly, in the field surveys two 500-mL water samples were collected in two separate bottles. The water in one bottle was treated with H_2SO_4 so as to reach a pH of 1–2; this water was used for NH_4^+ and TN measurements. The water in the other bottle was treated with HCl to reach a pH of 1–2 and stored for the measurement of NO_3^-. The two bottles were then immediately stored at the dark and at room temperature. N speciation (NH_4^+, NO_3^- and TN) analyses were conducted using standard spectrophotometric methods (UV-1201, Beifen-Ruilia Analytical Instruments, Ltd., Beijing, China) and performed within 7 days after sampling. Briefly, the NH_4^+, NO_3^- and TN concentrations in the water were determined using Nessler's reagent spectrophotometry (HJ 535-, 2009), ultraviolet spectrophotometry (HJ/T 346-, 2007) and alkaline potassium persulfate digestion UV spectrophotometry (HJ 636-, 2012),

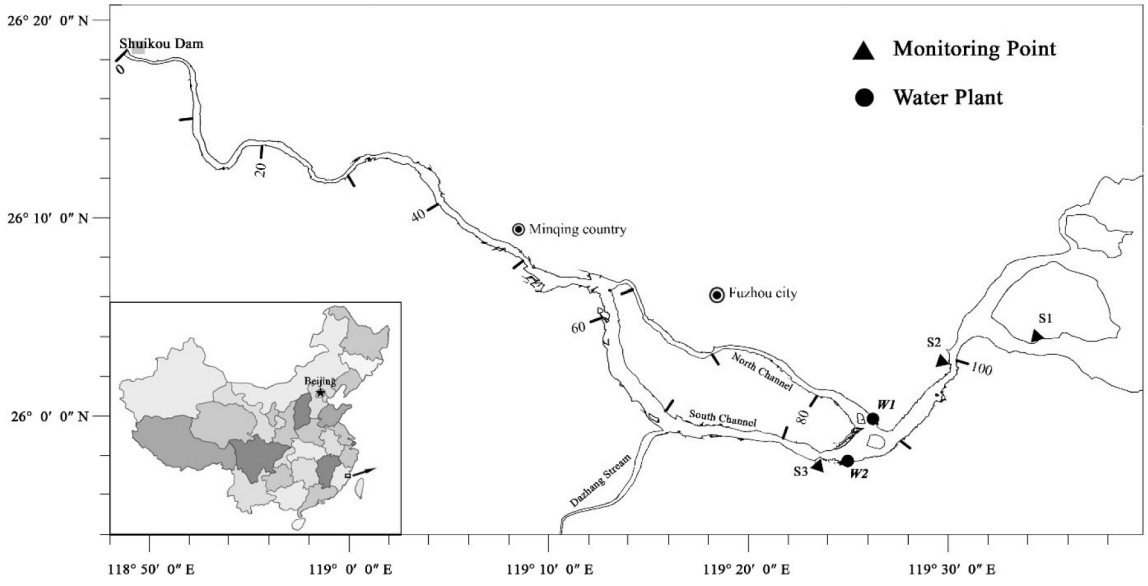

Fig. 1. Map of the Minjing River and the sampling sites surveyed in this study. The inset shows the location of the river in southeastern China.

respectively. All N speciation determinations were carried out in technical duplicates. The links to each of the standard methods are provided in the References.

2.3. Experimental setup

Based on the field surveys, water and sediments were collected to simulate saltwater intrusion in a tidal reach on July 20 2018 and monitor the related changes in N speciation and microbial succession under different salinity conditions. The collected water and sediments were immediately used to prepare the experiment after being transported to the Lab. Two annular flow tanks with a 2-m straight flume and 0.4-m round flume were prepared (Fig. 2). The first tank was used for salt addition and the other as a control. In both, 5 cm of sediment was placed at the bottom of the tanks followed by 20 cm of overlying water. The tanks were left for 24 h prior to the experiment to minimize agitation at the onset. A wave-making device with blade rotation (SW-15, Jebao Electronic Appliance Ltd., Guangdong, China) was used to agitate the overlying water at a speed of 0.1 cm/s, resulting in a circulatory wave at the surface. The 4:1 (v:v) ratio of natural water to sediment minimized sediment disturbance due to water flow. The water used to fill the two tanks had a salinity of 0.06. In the salt-treated (experimental) tank, a siphon was used to pump up ~1 L of surface water from the tank into a container, after which salt (pure NaCl) was added and allowed to dissolve. The method was designed to ensure that no microbial communities were introduced into the experimental system. The salt solution was then gently added to the experimental tank and the contents of the microcosm were homogenized using the wave-making device. The four salt pulses in the experimental tank (ET) resulted in salinities of 1.7, 15.1, 22.0 and 34.8. The microcosms without salt addition served as the control tank (CT). The salt pulses were carried out after different time intervals depending on the stability of the NH_4^+ concentration. Initially, the two tanks were kept under the same conditions without salt addition for 11 days. Salt was added to the ET when the difference in the NH_4^+ concentrations measured on two consecutive days did not exceed 10% of the relative error. NH_4^+ was chosen as the monitoring index for the salt pulse manipulation because not only is it sensitive to salinity changes, it is also a key pollutant in the total discharge in China. The two tanks were incubated under natural outdoor setting but were prevented from the rain precipitation with a rain shelter.

2.3.1. Measurement of N speciation

For the two microcosms (CT and ET), 250 mL of water was collected every 24 h from each of the three sampling taps and used to determine N speciation. The water samples from the three taps of each microcosm served as biological replicates. The samples used to determine N speciation and the concentrations of NH_4^+, NO_3^- and TN were handled as described for the field surveys. Additionally, dissolved N_2O was measured by gas chromatography (GC-2014, Shimadzu, Kyoto, Japan) using a gas-stripping method (Zhang et al., 2006; Tong et al., 2013). Water from the original source and with the same salinity (0.06) was added to the microcosms after each sampling such that the water volume stayed constant throughout the experiment and ensured the same degree of sediment oscillation in the two tanks.

2.3.2. Sample collection and DNA extraction

Microbially mediated N transformations were followed by assessing nitrification, denitrification and DNRA activities. In addition to determining N speciation in those processes, we quantified the abundances of the functional genes involved in nitrification (*amoA-AOA, AOB and nxrA*), denitrification (*narG*, *nirK*, *nirS* and *norB*) and DNRA (*napA* and *nrfA*) as a function of total bacterial and archaeal abundances as determined by in a 16S rRNA analysis (Supplementary Table S2).

Water samples were collected from each of the three sampling taps of the two microcosms and pre-filtered through 0.7-μm pore-size, 50-mm membrane filters (Millipore, Darmstadt, USA) in order to remove large sediment particles. The pre-filtered water was then filtered through 0.45-μm pore-size, 50-mm membrane filters to collect cells from the overlying water. Owing to a minority of sediment particle suspension in the water the 0.45-μm rather than 0.22-μm pore-size filters were chosen in order to minimize clogging on the filters. The filters were immediately stored at −20 °C until they were used for DNA extraction. The same filtration procedure was carried out for the replicates representing the four salinity levels in the ET and for the single sample filtered from the initial water, for a total of nine samples.

Genomic DNA (gDNA) from the nine samples was extracted using the TIANamp soil DNA kit (Tiangen Biotech, Beijing) according to the manufacturer's instructions. The gDNA was purified using the TIANamp genomic DNA kit (Tiangen Biotech), quality checked by gel electrophoresis and Nanodrop 2000 spectrophotometry (Thermo Fisher Scientific, DE, USA) and then stored at −20 °C until needed. The concentrations of the extracted DNA from all samples are reported in Supplementary Table S3.

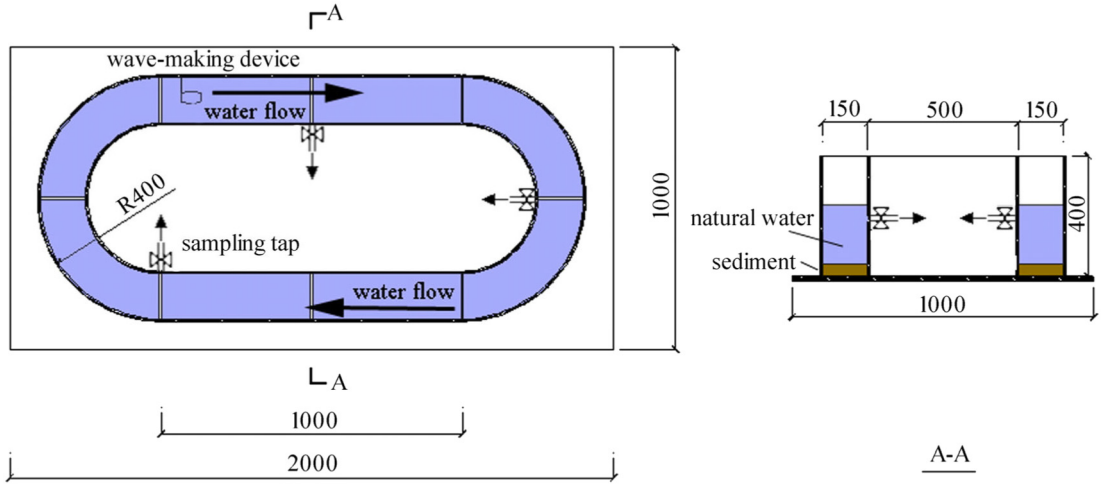

Fig. 2. Configuration of the circular experimental tank. Large figure represents top-down view (i.e., cross-section) of the tank. Small figure represents side view (i.e., longitudinal section) of the tank. The tank was 400 mm in diameter, 2000 mm in length, 1000 mm in width (shown the in large figure) and 400 mm in height (shown in the small figure). In addition, the area in which water flows was150 mm in width (shown in the small figure). The tank was equipped with three sampling taps and a wave-making device. The water flow (in blue) was in the clockwise direction. Natural water (in blue) and sediment (in brown) were incubated in microcosms. The ratio of the volume of natural water to that of sediment was 4:1, which assured a very minimal degree of sediment disturbance due to water flow. (For interpretation of the references to color in this figure legend, the reader is referred to the web version of this article.)

2.3.3. Quantification of functional genes by quantitative PCR (qPCR)

To explore the N transformation processes at the gene level, the above-mentioned functional genes of interest were PCR-amplified using the primers listed in Supplementary Table S2. A number of procedures were applied to standard preparation for each of the 10 genes, including initial PCR and excision of DNA fragments for synthetic gene plasmid cloning and plasmids' extraction (see detailed methods for standard preparation in the Supplementary Text). For each sample, the DNA template later used for qPCR was 10-fold diluted from the original concentration. The amplification was performed in 20-μL reaction mixtures containing 10 μl of SYBR Premix Ex TaqII (Takara BioInc. Japan), 0.5 μL of the forward primer, 0.5 μL of reverse primer and 2 μL of DNA template. The qPCR was carried out in 96-well plates using the Light Cycler ABI7500 (Applied Biosystems, Invitrogen, USA), and the following PCR conditions: 30 s at 95 °C, 40 cycles of 95 °C for 5 s and 60 °C for 40 s. Technical triplicates were performed for each set of samples. Supplementary Table S2 and Fig. S2 summarize the efficiencies and amplification specificity of qPCR assays for all genes.

2.4. Statistical analyses

A Mann-Whitney *U* test was used to assess the difference in the concentrations of each N species in the ET vs. the CT at each salt pulse manipulation. Pearson's correlation was used to explore the relationship between N concentrations, the relative abundance of functional genes and salinity. All statistical analyses were performed using SPSS 17.0 (SPSS Inc., Chicago, IL, USA) and the R environment (v.3.6.1). The data were visualized using the ggplot2 package in R (v.3.2.1; Wickham et al., 2019).

3. Results

3.1. Changes in N speciation following salinity intrusions in a field survey

On-site surveys in August 2017 and 2018 showed that stations S1 and S2 were subject to salt intrusions whereas station S3 was not. The salinity at S2 ranged from 0.03 to 2.05 in 2017 (Fig. 3A), while the salinities ranged from 0.35 to 3.93 at S2 and 5.73 to 9.25 at S1 in 2018, respectively (Fig. 3B and C). The depth profiles of salinity in both 2017 and 2018 revealed that salt stratification occurred when the salinity rose (Fig. 3). The salinity lamination at S1 and S2 ranged from 0.01 to 10, consistent with the findings of Liu et al. (2018). Thus, stations S1 and S2 represented partially mixed tidal reaches.

3.1.1. Temporal variations of N speciation during ebb and flood tides

On August 30, 2017, salinity at S2 remained between 0.03 and 0.04 from 8:00 until 14:00 and then increased to 2.05 at the final timepoint of 18:00 (Fig. 3A), reflecting the timing of the ebb and flood tides within a day, respectively. During the ebb tide, the concentrations of NH_4^+ (0.38 mg/L) and TN (1.53 mg/L) declined, whereas the NO_3^- concentration (0.68 mg/L) increased. However, the concentrations of all three species tended to be higher during the flood tide than during the ebb tide, with temporal variations in the patterns of each N form during the latter period. On August 22, 2018 the salinity at stations S1 and S2 decreased at the onset of monitoring and then rose, with 14:00 h again marking the transition from ebb tide to flood tide (Fig. 3B & C). The salinity fluctuation was more pronounced at S2 than at S1. The concentrations of NH_4^+, NO_3^- and TN varied during ebb tide (8:00–14:00) but without a clear trend among the three N forms. By contrast, during the flood tide, the concentrations of these N forms at S2 increased with increasing salinity, reaching highest values at the end of the monitoring period (18:00) (1.36, 1.27 and 2.98 mg/L, respectively; Fig. 3B). Similar changes in the concentrations of NH_4^+ and TN were determined in the 2013 field survey (Supplementary Fig. S1).

3.1.2. Spatial variations in N speciation among the three stations

Although salinity from S3 to S1 consistently increased following the transition from ebb tide to flood tide, the changes in NH_4^+, NO_3^- and TN differed between sites (Table 1). Thus, at ebb tide, all three N forms increased from S3 to S2 and declined at S1 (Table 1). A similar trend was observed for TN and NO_3^- at flood tide, but the concentration of NH_4^+ increased slightly from S2 to S1 in 2017 and rose from S3 to S1 in 2018.

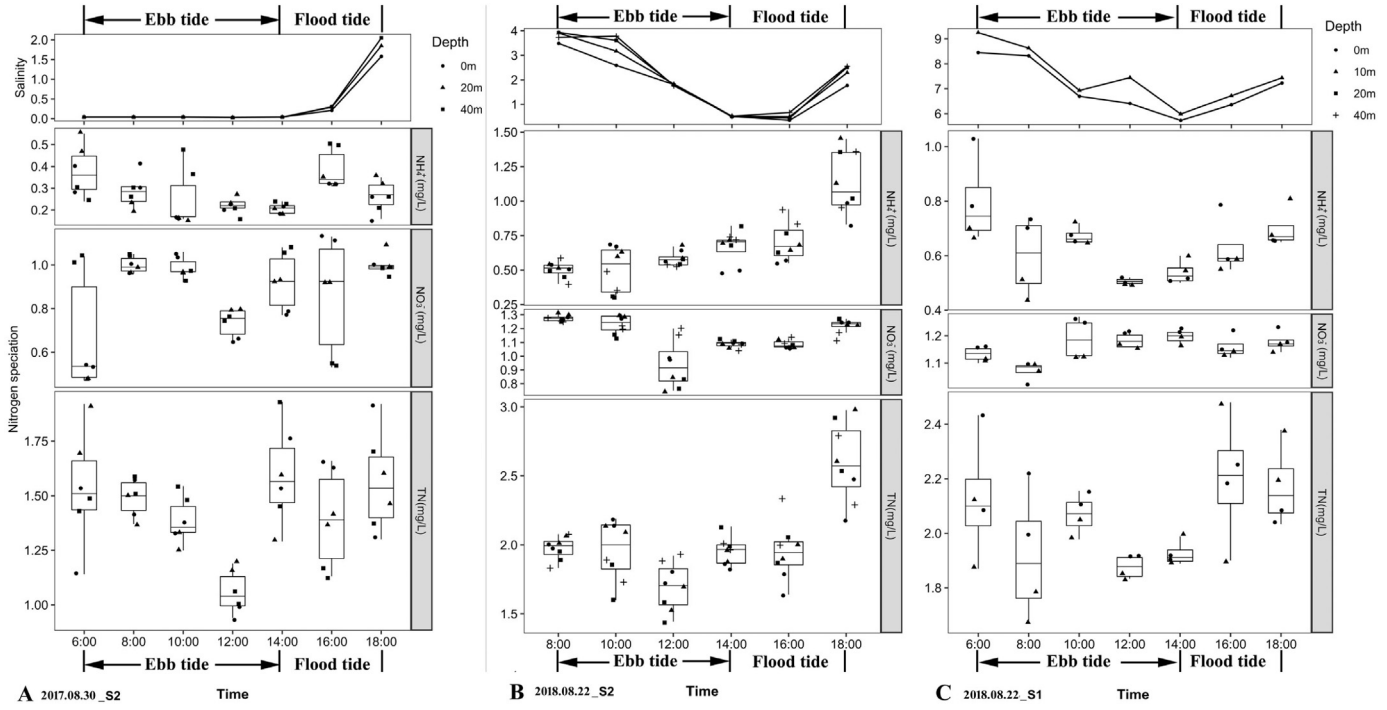

Fig. 3. Changes in salinity and the concentrations of NH_4^+, NO_3^- and TN during saltwater intrusion events in the field investigations A) on 30 August 2017 at S2 and on 22 August 2018 at B) S2 and (C) at S1. The boxplots show the overall trend (i.e., median of salinity and N speciation determined at different depths).

Table 1
Spatial distribution of nitrogen speciation under ebb tide and flood tide as determined in field investigations. The data are presented as the mean ± SD.

Time	Tide	Station	TN (mg/L)	NH_4^+ (mg/L)	NO_3^- (mg/L)	Salinity
2017.8	Ebb tide (8:00)	S3	1.01 ± 0.07	0.33 ± 0.06	0.67 ± 0.28	0.04 ± 0.00
		S2	1.52 ± 0.46	0.42 ± 0.25	0.87 ± 0.16	0.27 ± 0.05
		S1	1.21 ± 0.42	0.28 ± 0.18	0.75 ± 0.28	3.15 ± 0.12
	Flood tide (18:00)	S3	1.26 ± 0.13	0.29 ± 0.06	0.83 ± 0.16	0.04 ± 0.00
		S2	1.95 ± 0.30	0.22 ± 0.06	0.87 ± 0.29	1.75 ± 0.31
		S1	1.65 ± 0.27	0.26 ± 0.13	0.72 ± 0.23	4.54 ± 0.74
2018.8	Flood tide (8:00)	S3	1.42 ± 0.19	0.40 ± 0.04	0.88 ± 0.02	0.08 ± 0.01
		S2	1.95 ± 0.15	0.50 ± 0.04	1.26 ± 0.06	3.80 ± 0.28
		S1	1.89 ± 0.34	0.58 ± 0.11	1.12 ± 0.04	8.39 ± 0.35
	Ebb tide (14:00)	S3	1.32 ± 0.13	0.46 ± 0.05	0.73 ± 0.07	0.05 ± 0.00
		S2	2.06 ± 0.33	0.62 ± 0.10	1.24 ± 0.33	0.53 ± 0.10
		S1	1.89 ± 0.17	0.52 ± 0.07	1.18 ± 0.08	5.86 ± 0.13

3.2. Changes in N-speciation and gene abundance in a salt-addition experiment

3.2.1. N speciation changes under different salinity conditions

Overall, at low salinities (0.06 and 1.7) similar trends were observed for all N species in the experimental and control tanks whereas at high salinities (15.1, 22.0, and 34.8) the changes in the concentration of each N form were very large (Fig. 4). In the CT, the NH_4^+ concentration changed only slightly over time. The concentrations of NH_4^+ in the ET increased moderately after the first salt addition resulting in a salinity of 1.7 the concentration compared to the CT. The corresponding and significant increase in the NH_4^+ following the salt additions was also observed at the later stage of the experiment (Mann-Whitney *U* test, all $P < 0.05$, Fig. 4A). The concentrations of NO_3^- and TN were similar in the two tanks at low salinities but increased steadily in both before the first salt pulse on day 19 (Fig. 4B and C). However, after day 19 the salt pulses resulted in a significantly lower NO_3^- concentration in the ET than in the CT ($P < 0.05$, Fig. 4B). The TN concentrations in the ET at salinity pulses of 15.1 and 34.8 were significantly higher than in the CT ($P < 0.05$; Fig. 4C). In contrast to NH_4^+, NO_3^- and TN, the N_2O concentration increased following each salt addition ($P < 0.05$) but remained stable in the CT (Fig. 4D).

3.2.2. Changes in the abundances of functional genes under different salinity conditions

The relative abundance of each functional gene was estimated with respect to the absolute abundance of the 16S rRNA gene (Fig. 5 A; Supplementary Table S4). A decrease in 16S rRNA gene abundances was

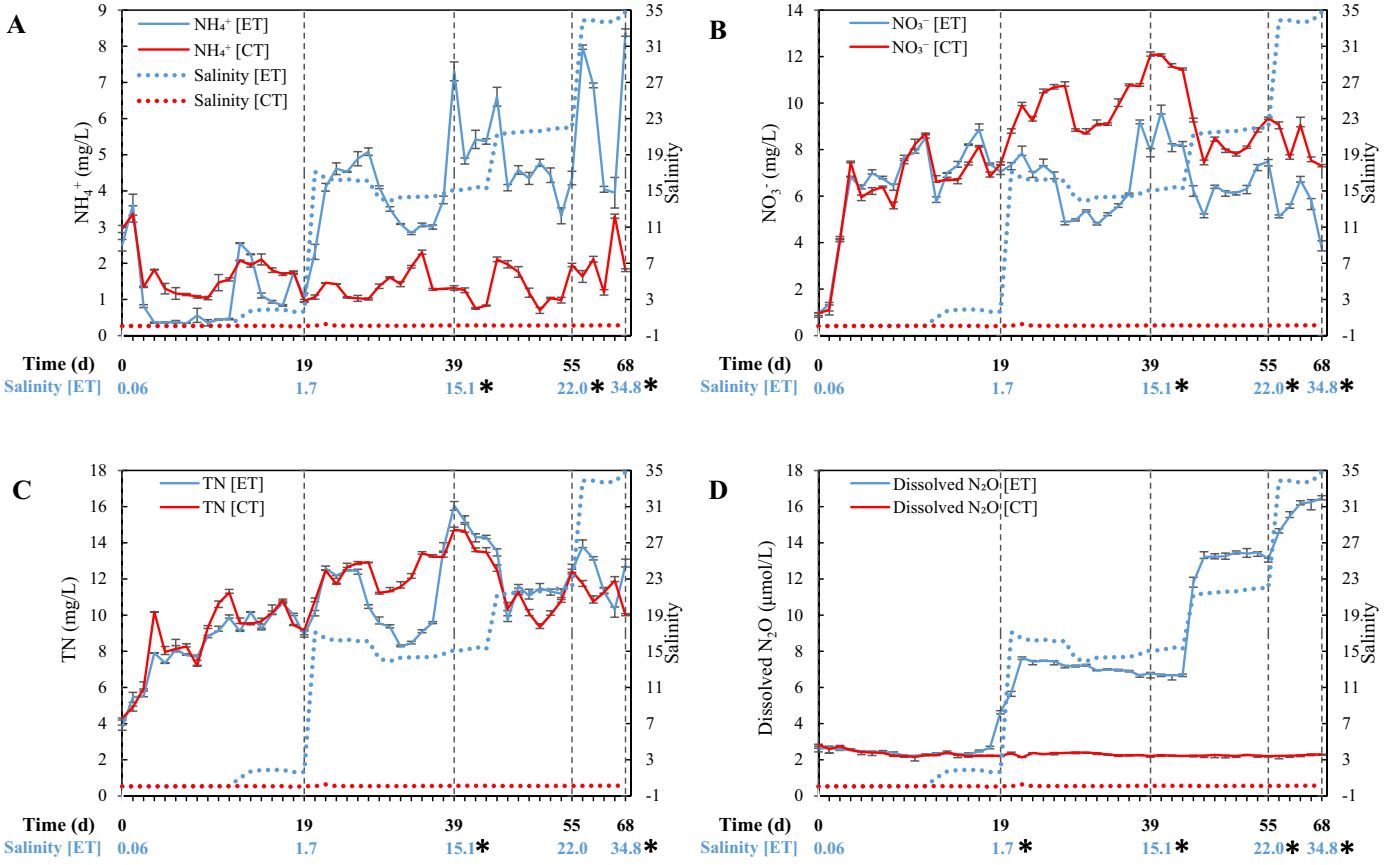

Fig. 4. Changes in nitrogen speciation following salt pulses. 'ET' represent the experimental tank with salt addition, as indicated in blue, while 'CT' represent the control groups without salt addition, as indicated in red. Salinity is indicated in blue for experimental tanks at each salt pulse event at the bottom of each figure, while control salinity was 0.06 for control tanks over time. Significance code: *$P < 0.05$ in a Mann-Whitney *U* test. (For interpretation of the references to color in this figure legend, the reader is referred to the web version of this article.)

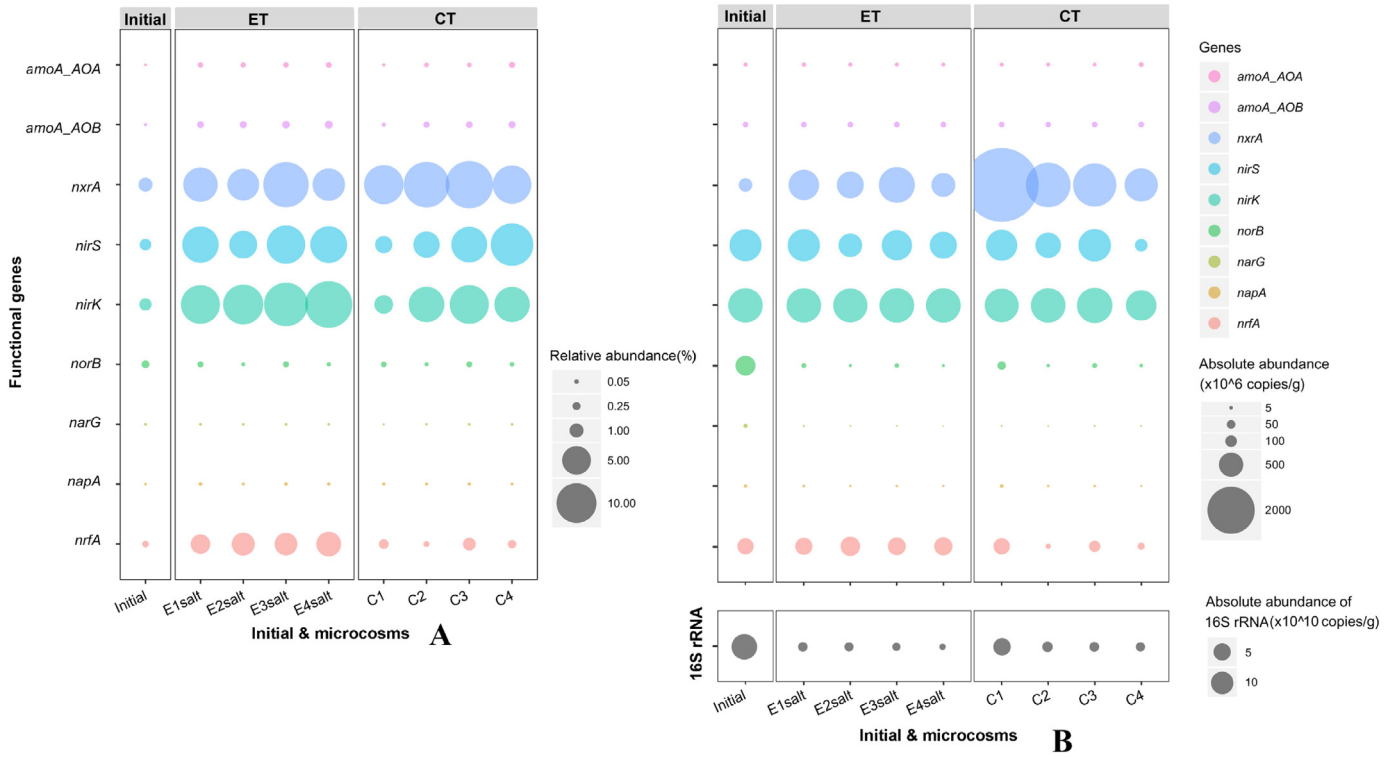

Fig. 5. Changes in the relative (A) and absolute (B) abundances of functional genes following salt pulses. 'Initial' represents the initial stage of the experiment, in which the salinity was 0.06. 'ET' represents the experimental tank with salt addition, while 'CT' represents the control tank without salt addition. 'E1salt', 'E2salt', 'E3salt' and 'E4salt' indicate the four salt pulses over time, referring to salinities of 1.7, 15.1, 22.0 and 34.8, respectively. 'C1', 'C2', 'C3' and 'C4' are the control for each of the salt addition events. The size of the circle corresponds to the level of gene abundance.

observed in the ET with increasing salinity, suggesting a negative impact of increasing salinity on the size and possibly also the overall composition of the microbial community. At the initial stage of the experiment, *nxrA* was highly abundant (relative abundance of 1.01%), whereas the eight other N functional genes each accounted for <1%. The relative frequency of *nirK*, involved in denitrification, was high in all four ET samples and especially following the largest salt addition, with a maximal relative abundance of 14.14% at a salinity of 34.8 (Supplementary Table S4). The second and third most abundant genes in the ET were *nxrA* and *nirS*, required for nitrification and denitrification, respectively (Fig. 5A). At a salinity of 22.0, these two genes accounted for 13.12% and 9.20% of the relative abundance (Supplementary Table S4). The other genes involved in nitrification and denitrification (*amoA-AOA*, *amoA-AOB*, *norB* and *narG*) were underrepresented in each sample (relative abundance <1%) (Fig. 5A). In the case of DNRA, the *nrfA* gene was enriched in response to salt addition and was the fourth most abundant gene in the ET (Fig. 5A), increasing from 2.14% to 3.60% (Supplementary Table S4). Overall, the abundances of nitrification genes in the ET vs. the CT declined by 0.08- to 0.52-fold whereas the abundances of denitrification genes increased 0.17- to 3.88-fold (Supplementary Table S4). A similar but more pronounced response was observed for the DNRA genes, the abundance of which increased 2.64- to 24.38-fold.

Absolute abundances, expressed as gene copy numbers, were determined as a proxy for quantitative measurements of functional genes (Fig. 5B and see Supplementary Table S5 'absolute abundance'). Accordingly, the absolute abundance of *nxrA* decreased in response to the salt additions in the ET but also over time in the CT (Fig. 5B). The absolute abundance of the *nirK* gene remained similar ($1.02–1.05 \times 10^9$ copies/g) across all samples in the ET (Fig. 5B and Supplementary Table S5), despite the tendency of an increase in the salt-added treatments as determined based on the relative abundances. The absolute abundance of the *nirS* gene increased over time but there was a reduction in the ET compared with the CT (Fig. 5B). The *nrfA* gene was enriched in the ET, with an abundance one order of magnitude greater than that in the CT (Fig. 5B). In both microcosms the absolute abundances of *amoA-AOA*, *amoA-AOB*, *norB*, *narG* and *napA* were lower than those of the other studied N genes (Fig. 5B).

3.3. Correlation between N concentrations, functional genes and salinity

The Pearson's correlation analysis revealed that salinity exerted a more positive effect on DNRA ($R = 0.881$, $P < 0.01$) than on denitrification but it negatively influenced the abundances of genes related to nitrification and of the 16S rRNA genes. The concentrations of NH_4^+ and dissolved N_2O correlated positively with salinity ($R = 0.90$ and 0.98, respectively; $P < 0.01$, Table 2). The higher NH_4^+ concentration tended to be correlate with the higher relative abundances of the DNRA genes ($R = 0.82$, $P < 0.01$), which indicated that microorganisms carrying this gene modulated the concentrations of NH_4^+ in response to changes

Table 2
Pearson's correlation coefficients for N speciation and the relative abundances of functional genes involved in N transformation in the microcosms. For nitrification, denitrification and DNRA, the relative gene abundances were aggregated for each process, except in the cases of the 16S rRNA gene in which only one gene was surveyed.

Factor	Nitrification genes	Denitrification genes	DNRA genes	16S rRNA gene	Salinity
TN	0.57	0.56	0.46	−0.81**	0.41
NH_4^+	−0.27	0.43	0.82**	−0.23	0.90**
NO_3^-	0.84**	0.25	−0.16	−0.68*	−0.28
Dissolved N_2O	−0.04	0.61	0.88**	−0.34	0.98**
Salinity	−0.08	0.58	0.88**	−0.34	1

Significance codes: ** = $P < 0.01$, * = $P < 0.05$. The targeted functional genes and their related pathways: *amoA-AOA*, *-AOB* and *nxrA* in nitrification, *narG*, *nirK*, *nirS* and *norB* in denitrification and *napA*, *nrfA* in DNRA.

in salinity. The relative abundances of nitrification genes correlated positively with NO_3^- levels ($R = 0.84$, $P < 0.01$), but negatively, albeit not significantly, with TN, NH_4^+ and dissolved N_2O levels. The transformation of each N form correlated negatively with 16S rRNA gene abundance, with significant relationships determined for TN ($R = 0.81$, $P < 0.01$) and NO_3^- ($R = 0.68$, $P < 0.05$). By contrast, the concentrations of all N forms correlated positively with denitrification gene abundances.

4. Discussion

Salinization of riverine systems due to climate change and anthropogenic activities has threatened their water quality (Herbert et al., 2015; Mansour et al., 2018). Changes in salinity are a major environmental stressor that trigger biogeochemical and microbial responses (Herbert et al., 2015). N cycling is a critical ecosystem service in aquatic systems and water quality is in part determined by the types of N transformation. Our 2-year field surveys of the Mingjiang River allowed us to investigate N speciation during ebb and flood tides. Based on our observations, we then conducted a controlled laboratory study simulating the salt intrusion that occurred in the natural tidal reaches of the river and assessed both N transformation and the abundance of functional genes related to N transformation.

Our field data obtained from August 2017 and 2018 generally showed that temporal changes in all N forms varied with time during ebb tide but not during flood tide, pointing to the important role of salinity in N speciation during flood tides. This is most likely because upstream pollution loading during the former period whereas the intrusion reach was restrained during the latter one (Xie et al., 2017b). As such, the effect of various pollution sources on N speciation during flood tides was expected to be small and that of salinity much greater. This idea was supported by the earlier year surveys conducted in the low tide and high tide events during the flood tide in our previous surveys (Supplementary Table S1). We found that under high salinity during the high tide event the concentration of NH_4^+ increased 18–60% whereas the concentrations of NO_3^- and TN fluctuated. At the spatial scale, the concentrations of all N forms were higher at S1 and S2 than S3, and similar trends were observed for differences in salinity among the three sites. This result suggests that spatial variability of N speciation correlates with salinity in the Mingjian River.

4.1. Impact of increasing salinity on NO_3^-

In both the field surveys and the laboratory experiment, high salinity had a negative impact on NO_3^- concentrations, which is consistent with the results of previous studies conducted in coastal wetlands (Marks et al., 2016). In that study, the authors were able to attribute the reduction of NO_3^- to an increase in denitrification induced by the increased salinity (Marks et al., 2016). In our study the positive correlation between the NO_3^- concentration and gene abundances, was significant only for nitrification, not for denitrification. The abundance of *nxrA* gene declined in response to salt addition and was lower than in the control (no salt addition). Previous studies have shown that the majority of the reduction in nitrification was due to the low activity of the nitrifiers involved in the first stage of nitrification, in which NH_4^+ is oxidized to NO_2^- by ammonia-oxidizing prokaryotes (*AOA* and *AOB*) (Zhang et al., 2015; Breuillin-Sessoms et al., 2017). In our microbial system, the abundances of the *amoA-AOA* and *-AOB* genes did not differ between the control and experimental tanks (Fig. 5; Supplementary Table S4). However, the diversity loss of active ammonia oxidizers over time and during salt pulse events might have resulted in no differences in the *amoA* abundances of the microcosms with and without salt addition at the end of the experiment, as they are generally thought to be sensitive to increasing salinity (Sanders and Laanbroek, 2018). Also, the increase in salinity more likely led to a suppression of the second step of microbial nitrification. Our results support existing studies highlighting the importance of *nxrA*-expressing (nitrite-oxidizing) bacteria in the efficiency of nitrification under shifting salinity conditions. Moreover, DNRA in which NO_3^- was reduced to NH_4^+ was stimulated by increasing salinity as indicated by a positive correlation between the abundance of *nrfA* and salinity, which provided evidence of an alternative pathway to the NO_3^- reduction that was favored at high salinity. We observed that increased salinity led to an increase in abundances of both *narG* for denitrification and *napA* for DNRA and such increase was more pronounced in the latter process (Supplementary Table S4). This finding suggests that changes in salinity promotes partitioning of nitrate reductases for the two processes and DNRA can outcompete denitrification for nitrate reduction. Kraft et al. (2014) have showed that denitrification prevailed at short generation times of microbial communities, whereas ammonification was more successful at long generation times. Microbial communities in our microcosms may have been subjected to a carrying capacity, as indicated by a decrease over time in 16S rRNA gene both in the CT and ET (Fig. 5B). That low capacity is indicative of long generation time in microbes, particularly toward the end of the experiment, i.e., a 68-day incubation. As such, the dominance of DNRA for nitrate reduction could have been attributed to the slow growth of microbes and experimental conditions, i.e., increasing salinity.

4.2. Impact of increasing salinity on dissolved N_2O

We studied the dissolved rather than the atmospheric form of N_2O because the former contributes to the total dissolved N in water (Mcmahon and Dennehy, 1999). We observed that salt addition significantly enhanced the dissolved N_2O concentration (Fig. 4D), with the most pronounced response occurring at the highest salinity. Denitrification is not necessarily an anoxic process; it does occur in a variety of microaerobic conditions (i.e., Gao et al., 2010; Coban et al., 2015). Our experimental system can be regarded as an oxic environment, because the constant water flow generated moderate levels of dissolved oxygen in the microcosms (Supplementary Table S6). At the same time, the increasing salinity in the microcosms would have increased the ionic concentrations in the water overlying the sediment, thus changing the chemical equilibrium and mineral solubility over a short time scale (days to weeks), in turn altering the redox state in the tank. These redox oscillations would have altered the activities of denitrifying bacteria or different members of the microbial community in driving metabolic processes. Together, the increasing salinity and accompanying changes in the redox state of the system seem to have stimulated denitrification, as the abundances of genes required for this process increased following salt addition.

The coincidence of increases in N_2O concentration and the salt pulses in the ET raises the question whether denitrification or nitrification had the larger contribution to N_2O production (de Wilde and de Bie, 2000). If nitrification in the water column of the ET contributed to this increase, then the proportion of *amoA* abundances should have increased as well, but this was not the case. Furthermore, it seems implausible that nitrification in surface sediments or sedimentary denitrification dominated N_2O formation. If N_2O fluxes at the sediment-water interface were the product of both processes, then the N_2O concentration should also have increased in the control. However, in the absence of salt addition the N_2O concentration remained low throughout the experiment (Fig. 4D). In addition, raises in the N_2O concentration in response to the increasing salinity in the ET were durative rather than punctuated, suggesting the progressive accumulation of N_2O during the denitrification process. The activity of N_2O reductase, which reduces N_2O to N_2 during N transformation, was shown to be sensitive to high salinity (Menyailo et al., 1997; Tsuneda et al., 2005) such that N_2O reduction is inhibited (Laverman et al., 2007). Most likely, the salt pulse events in the ET induced a salting-in effect, in which the increased ionic strength of a solution increases the solubility of a solute; thus, in our study the solubility of the accumulated N_2O in the water would have increased following salt pulse.

4.3. Impact of increasing salinity on NH_4^+

Previous work showed a decrease in nitrification at elevated salinities, and the opposite for DNRA (Giblin et al., 2010; Wang et al., 2018). In our field surveys, the higher NH_4^+ levels tended to be correlate with increasing salinity during salt intrusions, which is consistent with earlier findings reported by Laverman et al. (2007). This was also convincingly demonstrated in our experiment, in which large increases in the NH_4^+ concentration occurred following salt pulse. Autotrophic nitrification may not have been sufficient for the removal of NH_4^+ in the microcosms. Instead, the significant positive correlation between the NH_4^+ concentration and *nrfA* abundance suggested that the increase in NH_4^+ resulted from the reduction of NO_3^- in DNRA.

The increased NH_4^+ concentrations in the microcosms following salt addition may also have been due to inputs from the sediments. Previous work showed that in a coastal freshwater sediment an increase in bottom-water salinity led to releases of NH_4^+ and dissolved organic carbon (Laverman et al., 2007). Also, in high-saline environments, mineralization processes are increased and accelerate the release of NH_4^+ from the sediments (Xie et al., 2017a; Luo et al., 2019). Either mechanism may thus, at least temporarily, increase the efflux of NH_4^+ from the sediment to the surface water. In our study this transient release of NH_4^+ would have accounted for the large fluctuations in NH_4^+ that accompanied the salt pulses. When NH_4^+ in the water reached its highest level, the imbalance between the sediment and overlying water would have favored sediment adsorption (Hou et al., 2003).

4.4. Mechanisms and implications of salt intrusion on N-cycle

We have showed that nitrification and denitrification respond differently to increased salinity, as evidenced by differences in the abundances of dominant genes, that the coupling of these two microbial processes alters N transformation in the tidal reach. We also highlight the role of DNRA as an important pathway of NH_4^+ production in the N cycle under saltwater intrusion scenarios. Here, we propose a mechanistic framework to understand the impact of salt intrusion on N-cycling, as demonstrated in the graphical abstract. During salt intrusion to freshwater environments, progressively increasing salinity reduces nitrification efficiency due to suppression of growth of microorganisms carrying *amoA* encoding ammonia monooxygenase (Santoro et al., 2008; Sanders and Laanbroek, 2018) and *nxrA* encoding nitrite oxidoreductase, referred to as ammonia oxidizers and nitrite oxidizing bacteria. The lower abundances of two key genes in nitrification led to lower nitrifying capacity under oxic conditions, and NO_3^- production tends to be less efficient. Concomitantly, the increased salinity facilitates NO_3^- reduction in denitrification and DNRA, with partitioning of NO_3^- greater in the latter process. Besides for the microbial intrinsic growth and experimental conditions discussed above, presumably DNRA had taken an advantage of excess nitrate as electron acceptors under low conditions, i.e., water overlying the sediment, give that denitrification may have occurred aerobically in our microcosms, i.e., oxygen as an efficient electron acceptor (Chen and Strous, 2013). As a result, the higher NH_4^+ concentrations correlate with higher salinity. The increased NH_4^+ pools can stimulate the growth of phytoplankton which preferentially utilize NH_4^+ over other forms of IN, thereby exacerbating eutrophication in aquatic environments. On the other hand, the coupling of nitrification and denitrification under high saline conditions favors NO_2^- reduction to denitrification performance. As such, salinity tolerance of the nitrifiers and/or denitrifiers that carry (*nirK*/*nirS*) and nitric oxide reductase (*norB*) allows N_2O formation to happen, in addition to the 'salt-in effect' on the increased N_2O accumulation. Overall, the mechanisms of salt intrusion on N cycle encompass the complex interplay between N transformation of nitrification, denitrification and DNRA. We hypothesize that large and progressively changes in salinity accompanied with redox fluctuations exert the selective force on the nitrate and nitrite reductions and thus govern their dominance in DNRA and denitrification.

According to Henry's law (Henry, 1803), in which the amount of dissolved gas in a liquid is proportional to its partial pressure above the liquid, our study suggests that a high quantity of N_2O dissolved in water implies a strong possibility of its emission as a greenhouse gas during tidal events. Finally, the relations among NH_4^+, NO_3^- dissolved N_2O and related functional genes revealed by the present study provide a solid foundation for a comprehensive understanding of N cycling (including organic N, N_2 and the participation of genes other than those included in our study, such as *hzsA* and *nosZ*). Further work aimed at quantifying the expression of the full spectrum of genes involved in N transformation is crucial to determine whether freshwater environments under saltwater intrusion are a sink or a source of N_2O production and reduction.

4.5. Caveats and recommendations for future work

Confounding factors in the field, i.e., N inputs (Boynton et al., 2014; Bellmore et al., 2018) and sulfide concentrations (Giblin et al., 2010), were not captured in our laboratory experiment but in natural systems they may influence the variability in the TN concentration. Our experiment was designed to reproduce the salt pulse event while keeping other abiotic factors, such as pH, dissolved oxygen, temperature and water speed, constant. However, in most natural systems, saltwater intrusion carries salt- and oxygen-rich waters (Feistel et al., 2016). Their natural mixing introduces external sources of microbes that may compete with local microbial communities and thus modify local species diversity (Shen et al., 2018). Unknown nuances in local abiotic and biotic conditions and their interplay could have resulted in different trajectories of aquatic N speciation and therefore of N transformation as well. For instance, saltwater inflows can stimulate competition between heterotrophic bacteria, introduced by saltier, well-oxygenated water, and locally adapted nitrifying bacteria, particularly in the sediment (Middelburg and Nieuwenhuize, 2000). Further studies using more advanced molecular tools, such as stable isotope probing and NanoSIMS, will enable an in-depth analysis of the quantitative partitioning of N forms in transformation processes (Radajewski et al., 2000; Li et al., 2008).

5. Conclusions

Our field investigations and laboratory experiment showed that salt intrusion can have a profound impact on aquatic N speciation and transformation processes in tidal river water, especially during flood periods. High-saline conditions led to a decrease in the concentration of NO_3^- that mainly resulted from a decline in nitrification and a simultaneous increase in DNRA. The increase in salinity also promoted N_2O accumulation, mostly likely due to the increased water solubility of N_2O following a salt-in effect and to the inhibition of N_2O reductase activity. N_2O accumulation in the water was therefore dependent of the strength of the salt pulse. The increase in the NH_4^+ concentration after salt addition was attributed to DNRA processes. Taken together, our results demonstrate the feasibility of combining field and laboratory approaches to ascertain the effect of increasing salinity on aquatic N and to unravel the mechanisms that underlie the changes in N cycles. This knowledge is critical for guiding management efforts aimed at protecting already-limited freshwater resources and improving water quality in estuaries.

CRediT authorship contribution statement

Rongrong Xie: Conceptualization, Methodology, Writing - original draft, Visualization, Supervision.**Peiyuan Rao:**Investigation, Formal analysis, Data curation.**Yong Pang:**Conceptualization, Resources. **Chengchun Shi:**Resources, Funding acquisition.**Jiabing Li:**Investigation, Resources.**Dandan Shen:**Conceptualization, Data curation, Writing - original draft, Writing - review & editing, Supervision.

Declaration of competing interest

The authors declare that they have no known competing financial interests or personal relationships that could have appeared to influence the work reported in this paper.

Acknowledgments

This work was partially supported by the study abroad scholarship from the Department of Education, Fujian Province and Fujian university, China (2018071091); Science and Technology Planning Project of Fuzhou, China (2019-S-67). We gratefully acknowledge the support of K. C. Wong Education Foundation and the grant from German Academic Exchange Service (DAAD) to R. X.

Appendix A. Supplementary data

Supplementary data to this article can be found online at https://doi.org/10.1016/j.scitotenv.2020.138803.

References

Alcérreca-Huerta, J.C., Callejas-Jiménez, M.E., Carrillo, L., Castillo, M.M., 2019. Dam implications on salt-water intrusion and land use within a tropical estuarine environment of the Gulf of Mexico. Sci. Total Environ. 652, 1102–1112.
Barlow, P.M., Reichard, E.G., 2010. Saltwater intrusion in coastal regions of North America. Hydrogeol. J. 18, 247–260.
Bellmore, R.A., Compton, J.E., Brooks, J.R., Fox, E.W., Hill, R.A., Sobota, D.J., Thornbrugh, D.J., Weber, M.H., 2018. Nitrogen inputs drive nitrogen concentrations in U.S. streams and rivers during summer low flow conditions. Sci. Total Environ. 639, 1349–1359.
Boynton, W.R., Hodgkins, C.L.S., O'Leary, C.A., Bailey, E.M., Bayard, A.R., Wainger, L.A., 2014. Multi-decade responses of a tidal creek system to nutrient load reductions: Mattawoman creek, Maryland USA. Estuaries & Coasts 37, 111–127.
Breuillin-Sessoms, F., Venterea, R.T., Sadowsky, M.J., Coulter, J.A., Clough, T.J., Wang, P., 2017. Nitrification gene ratio and free ammonia explain nitrite and nitrous oxide production in urea-amended soils. Soil Biol. Biochem. 111, 143–153.
Camargo, J.A., Alonso, á., 2006. Ecological and toxicological effects of inorganic nitrogen pollution in aquatic ecosystems: a global assessment. Environ. Int. 32, 831–849.
Chen, J., Strous, M., 2013. Denitrification and aerobic respiration, hybrid electron transport chains and co-evolution. Biochim. Biophys. Acta 1827, 136–144.
Church, J. A., Clark, P. U., Cazenave, A., Gregory, J. M., Jevrejeva, S., Merrifield, M. A. Milne, G. A., Nerem, R. S., Nunn, P. D., Payne, A. J., Pfeffer, W. T., Stammer, D., Unnikrishnan, A., 2013. Sea-level rise by 2100. Science 342, 1445.
Coban, O., Kuschk, P., Kappelmeyer, U., Spott, O., Martienssen, M., Jetten, M.S., Knoeller, K., 2015. Nitrogen transforming community in a horizontal subsurface-flow constructed wetland. Water Res. 74, 203–212.
Damashek, J., Francis, C.A., 2018. Microbial nitrogen cycling in estuaries: from genes to ecosystem processes. Estuaries & Coasts 41, 626–660.
Das, S., Giri, S., Das, I., Chanda, A., Ghosh, A., Mukhopadhyay, A., Akhand, A., Choudhury, S.B., Dadhwal, V.K., Maity, S., Kumar, T.S., Lotliker, A.A., Mitra, D., Hazra, S., 2017. Nutrient dynamics of northern Bay of Bengal (nBoB) - emphasizing the role of tides. Reg. Stud. Mar. Sci. 10, 116–134.
Dong, L.F., Sobey, M.N., Smith .J., C, Rusmana, Phillips, W., Stott, A., et al., 2011. Dissimilatory reduction of nitrate to ammonium, not denitrification or anammox dominates benthic nitrate reduction in tropical estuaries. Limnol. Oceanogr. 56, 279–291.
Feistel, S., Feistel, R., Nehring, D., Matthäus, W., Nausch, G., Naumann, M., 2016. Hypoxic and Anoxic Regions in the Baltic Sea, 1969–2015. Meereswiss. Ber., Warnemünde, p. 100.
Franklin, R.B., Morrissey, E.M., Morina, J.C., 2017. Changes in abundance and community structure of nitrate-reducing bacteria along a salinity gradient in tidal wetlands. Pedobiologia 60, 21–26.
Gao, H., Schreiber, F., Collins, G., Jensen, M.M., Kostka, J.E., Lavik, G., de Beer, D., Zhou, H.Y., Kuypers, M.M.M., 2010. Aerobic denitrification in permeable Wadden Sea sediments. ISME J. 4, 417–426.
GB3838, 2002. Environmental Quality Standards for Surface Water. Standard Press of China, Beijing http://bz.mee.gov.cn/bzwb/shjbh/shjzlbz/200206/t20020601_66497.shtml.
Giblin, A.E., Weston, N.B., Banta, G.T., Tucker, J., Hopkinson, C.S., 2010. The effects of salinity on nitrogen losses from an oligohaline estuarine sediment. Estuaries & Coasts 33, 1054–1068.
Giblin, A.E., Tobias, C.R., Song, B., Weston, N., Banta, G.T., Rivera-Monroy, V.H., 2013. The importance of dissimilatory nitrate reduction to ammonium (DNRA) in the nitrogen cycle of coastal ecosystems. Oceanography 26, 124–131.
Helali, M.A., Zaaboub, N., Oueslati, W., Added, A., Aleya, L., 2016. Nutrient exchange and oxygen demand at the sediment–water interface during dry and wet seasons off the Medjerda River Delta (Tunis Gulf, Tunisia). Environ. Earth Sci. 75, 25.
Henry, W., 1803. Experiments on the quantity of gases absorbed by water, at different temperatures, and under different pressures. Proc. R. Soc. Lond. 93, 103–104.
Herbert, E.R., Boon, P., Burgin, A.J., Neubauer, S.C., Franklin, R.B., Ardón, M., Hopfensperger, K.N., Lamers, L.P.M., Gell, P., 2015. A global perspective on wetland salinization: ecological consequences of a growing threat to freshwater wetlands. Ecosphere 6, 1–43.
HJ 493, 2009. Water quality- technical regulation of the preservation and handling of samples. http://kjs.mee.gov.cn/hjbhbz/bzwb/jcffbz/200910/W020111114540735543139.pdf.
HJ 535, 2009. Water quality- determination of ammonia nitrogen-Nessler's reagent spectrophotometry. http://english.mee.gov.cn/Resources/standards/water_environment/method_standard2/201010/t20101027_196755.shtml.
HJ 636, 2012. Water quality- determination of total nitrogen-alkaline potassium persulfate digestion UV spectrophotometric method. http://english.mee.gov.cn/Resources/standards/water_environment/method_standard2/201206/t20120618_231805.shtml.
HJ/T 346, 2007. Water quality- determination of nitrate-nitrogen- ultraviolet spectrophotometry. http://english.mee.gov.cn/Resources/standards/water_environment/method_standard2/200807/t20080704_125017.shtml.
Hou, L., Liu, M., Jiang, H., Xu, S., Ou, D., Liu, Q., Zhang, B., 2003. Ammonium adsorption by tidal flat surface sediments from the Yangtze estuary. Environ. Geol. 45, 72–78.
Hu, Y., Wang, L., Fu, X., Yan, J., Wu, J., Tsang, Y., Le, Y., Sun, Y., 2016. Salinity and nutrient contents of tidal water affects soil respiration and carbon sequestration of high and low tidal flats of Jiuduansha wetlands in different ways. Sci. Total Environ. 565, 637–648.
Jia, R., 2011. Studies of Exchange Behavior of Nutrients on the Sediment-Water Interface in the Tidal Reach — Take Licun River in Qingdao as an Example (Dissertation from Ocean University of China (in Chinese).
Kieber, R.J., Long, M.S., Willey, J.D., 2005. Factors influencing nitrogen speciation in coastal rainwater. J. Atmos. Chem. 52, 81–99.
Kim, H., Ogram, A., Bae, H.S., 2017. Nitrification, anammox and denitrification along a nutrient gradient in the Florida Everglades. Wetlands 37, 391–399.
Kraft, B., Tegetmeyer, H.E., Sharma, R., Klotz, M.G., Ferdelman .G., T, Hettich, R.L., Geelhoed, J.S., Strous, M., 2014. The environmental controls that govern the end product of bacterial nitrate respiration. Science 345, 676–679.
Laverman, A.M., Canavan, R.W., Slomp, C.P., Cappellen, P.V., 2007. Potential nitrate removal in a coastal freshwater sediment (Haringvliet Lake, The Netherlands) and response to salinization. Water Res. 41, 3061–3068.
Li, L., Qin, S., Chen, Y., Zhao, X., Liu, J., Lu, Z., 2014. Response of active nitrogen to salinity in a soil from the Yellow River delta. Environmental Science 35, 2358–2364 (Chinese).
Li, T., Wu, T., Mazéas, L., Toffin, L., Guerquin-Kern, J., Leblon, G., Bouchez, T., 2008. Simultaneous analysis of microbial identity and function using NanoSIMS. Environ. Microbiol. 10, 580–588.
Liu, F., Hu, S., Guo, X., Niu, L., Cai, H., Yang, Q., 2018. Impacts of estuarine mixing on vertical dispersion of polycyclic aromatic hydrocarbons (PAHs) in a tide-dominated estuary. Mar. Pollut. Bull. 131, 276–283.
Luo, M., Huang, J.F., Zhu, W.F., Tong, C., 2019. Impacts of increasing salinity and inundation on rates and pathways of organic carbon mineralization in tidal wetlands: a review. Hydrobiologia 827, 31–49.
Mansour, I., Heppell, C.M., Ryo, M., Rillig, M.C., 2018. Application of the microbial community coalescence concept to riverine networks. Biol. Rev. 93, 1832–1845.
Marks, B.M., Chambers, L., White, J.R., 2016. Effect of fluctuating salinity on potential denitrification in coastal wetland soil and sediments. Soil Sci. Soc. Am. J. 80, 516–526.
Mcclung, G., Frankenberger, W.T., 1985. Soil nitrogen transformations as affected by salinity. Soil Sci. 139, 405–411.
Mcmahon, P.B., Dennehy, K.F., 1999. N_2O emissions from a nitrogen-enriched river. Environment Science & Technology 33, 21–25.
Menyailo, O.V., Stepanov, A.L., Umarov, M.M., 1997. The transformation of nitrous oxide by denitrifying bacteria in Solonchaks. Eurasian Soil Science 30, 178–180.
Middelburg, J.J., Nieuwenhuize, J., 2000. Nitrogen uptake by heterotrophic bacteria and phytoplankton in the nitrate-rich Thames estuary. Mar. Ecol. Prog. Ser. 203, 13–21.
Osborne, R.I., Bernot, M.J., Findlay, S.E.G., 2015. Changes in nitrogen cycling processes along a salinity gradient in tidal wetlands of the Hudson River, New York, USA. Wetlands 35, 323–334.
Pan, H., Pang, Y., Luo, J., Zhang, P., Xie, R., 2015. Influence of saltwater intrusion on water source land in downstream of Minjiang River based on EFDC. Journal of Water Resources & Water Engineering 26, 71–76 (in Chinese).
Pang, J., Yamato, M., Soda, S., Inoue, D., Ike, M., 2019. Nitrogen-cycling functional genes in brackish and freshwater sediments in Yodo River in Japan. Journal of Water and Environment Technology 17, 109–116.
Radajewski, S., Ineson, P., Parekh, N.P., Murrell, J., 2000. Stable-isotope probing as a tool in microbial ecology. Nature 403, 646–649.
Rahaman, S.M.B., Sarder, L., Rahaman, M.S., Ghosh, A.K., Biswas, S.K., Siraj, S.S., Huq, K.A., Hasanuzzaman, A.F.M., Islam, S.S., 2013. Nutrient dynamics in the Sundarbans mangrove estuarine system of Bangladesh under different weather and tidal cycles. Ecol. Process. 2, 29.
Ribas-Ribas, M., G'omez-Parra, A., Forja, J.M., 2011. Spatiotemporal variability of the dissolved organic carbon and nitrogen in a coastal area affected by river input: the north eastern shelf of the Gulf of C'adiz (SW Iberian Peninsula). Mar. Chem. 126, 295–308.
Rysgaard, S., Thastum, P., Dalsgaard, T., Sloth, C.N.P., 1999. Effects of salinity on NH_4^+ adsorption capacity, nitrification, and denitrification in Danish estuarine sediments. Estuaries 22, 21–30.
Sanders, T., Laanbroek, H.J., 2018. The distribution of sediment and water column nitrification potential in the hyper-turbid Ems estuary. Aquat. Sci. 80, 33.
Santoro, A.E., 2010. Microbial nitrogen cycling at the saltwater-freshwater interface. Hydrogeol. J. 18, 187–202.

Santoro, A.E., Francis, C.A., De Sieyes, N.R., Boehm, A.B., 2008. Shifts in the relative abundance of ammonia-oxidizing bacteria and archaea across physicochemical gradients in a subterranean estuary. Environ. Microbiol. 10, 1068–1079.
Schmidt, C.S., Richardson, D.J., Baggs, E.M., 2011. Constraining the conditions conducive to dissimilatory nitrate reduction to ammonium in temperate arable soils. Soil Biol. Biochem. 43, 1607–1611.
Shen, D., Langenheder, S., Jürgens, K., 2018. Dispersal modifies the diversity and composition of active bacterial communities in response to a salinity change. Front. Microbiol. 9, 2188.
Shen, J., Zhang, L., Di, H., He, J., 2012. A review of ammonia-oxidizing bacteria and archaea in Chinese soils. Front in Microbiology 3, 1–7.
Smith, C.J., Dong, L.F., Wilson, J., Scott, A., Osborn, A.M., Nedwell, D.B., 2015. Seasonal variation in denitrification and dissimilatory nitrate reduction to ammonia process rates and corresponding key functional genes along an estuarine nitrate gradient. Front. Microbiol. 6, 542.
Stoliker, D.L., Repert, D.A., Smith, R.L., Song, B., LeBlanc, D.R., McCobb, T.D., Conaway, C.H., Hyun, S.P., Koh, D., Moon, H.S., Kent, D.B., 2016. Hydrologic controls on nitrogen cycling processes and functional gene abundance in sediments of a groundwater flow-through lake. Environmental Science & Technology 50, 3649–3657.
Tong, C., Huang, J., Hu, Z., Jin, Y., 2013. Diurnal variations of carbon dioxide, methane, and nitrous oxide vertical fluxes in a subtropical estuarine marsh on neap and spring tide days. Estuaries & Coasts 36, 633–642.
Tsuneda, S., Mikami, M., Kimochi, Y., Hirata, A., 2005. Effect of salinity on nitrous oxide emission in the biological nitrogen removal process for industrial wastewater. J. Hazard. Mater. B119, 93–98.
UNESCO, 1985. The international system of units (SI) in oceanography. UNESCO Tech. Pap. Mar. Sci. 45, 43.
Wang, H., Gilbert, J.A., Zhu, Y., Yang, X., 2018. Salinity is a key factor driving the nitrogen cycling in the mangrove sediment. Sci. Total Environ. 631–632, 1342–1349.
Wang, K., Chen, J., Ni, X., Zeng, D., Li, D., Jin, H., Glibert, P.M., Qiu, W., Huang, D., 2017. Real-time monitoring of nutrients in the Changjiang estuary reveals short-term nutrient-algal bloom dynamics. J. Geophys. Res. 122, 5430–5903.
Wickham, H., Chang, W., Henry, L., Pedersen, T.L., Takahashi, K., Wilke, C., Woo, K., Yutani, H., 2019. Package 'ggplot2'. https://cran.r-project.org/web/packages/ggplot2/ggplot2.pdf.
de Wilde, H.P.J., de Bie, M.J.M., 2000. Nitrous oxide in the Schelde estuary: production by nitrification and emission to the atmosphere. Mar. Chem. 69, 203–216.
Xia, X., Liu, T., Yang, Z., Michalski, G., Liu, S., Jia, Z., Zhang, S., 2017. Enhanced nitrogen loss from rivers through coupled nitrification-denitrification caused by suspended sediment. Sci. Total Environ. 579, 47–59.
Xie, R., Li, J., Zhang, D., Huang, Q., Ding, X., Wu, C., 2017a. Salinity effects on the nitrogen mineralization in different wetland sediments of the Min river estuary. China Environ. Sci. 37, 2248–2254 (Chinese).
Xie, R., Pang, Y., Luo, B., Li, J., Wu, C., Zheng, Y., Sun, Q., Zhang, P., Wang, F., 2017b. Spatio-temporal variability in salinity and hydraulic relationship with salt intrusion in the tidal reaches of the Minjiang River, Fujian province, China. Environ. Sci. Pollut. Res. 24, 11847–11855.
Zhang, G., Zhang, J., Xu, J., Zhang, F., 2006. Distributions, sources and atmospheric fluxes of nitrous oxide in the Jiaozhou Bay. Estuar. Coast. Shelf Sci. 68, 557–566.
Zhang, Y., Chen, L., Dai, T., Tian, J., Wen, D., 2015. The influence of salinity on the abundance, transcriptional activity, and diversity of *AOA* and *AOB* in an estuarine sediment: a microcosm study. Appl. Microbiol. Biotechnol. 99, 9825–9833.
Zhou, M., Butterbach-Bahl, K., Vereecken, H., Bruggemann, N., 2017. A meta-analysis of soil salinization effects on nitrogen pools, cycles and fluxes in coastal ecosystems. Glob. Chang. Biol. 23, 1338–1352.